

On the goethite to hematite phase transformation

Stefano Gialanella · Fabrizio Girardi ·
Gloria Ischia · Ivan Lonardelli · Maurizio Mattarelli ·
Maurizio Montagna

Received: 28 December 2009 / Accepted: 18 March 2010 / Published online: 13 April 2010
© Akadémiai Kiadó, Budapest, Hungary 2010

Abstract This study deals with some microstructural and crystallographic aspects of the thermally induced transformation of goethite ($\alpha\text{-FeOOH}$) into hematite ($\alpha\text{-Fe}_2\text{O}_3$), occurring at about 300 °C. Powder specimens of goethite have been annealed in air at different temperatures, ranging from 200 °C up to 1,000 °C. The resulting products have been analyzed for a complete characterization of the changes brought about by the thermal treatments, using a multianalytical approach, based on: thermogravimetry, differential thermal analysis, transmission electron microscopy, Raman spectroscopy, and X-ray diffraction. At lower temperatures, the transition to hematite produces no important changes in size and shape of the original goethite grains. Recrystallization, and partial sintering, occurs only at temperatures in excess of 800 °C. The relevant evolution of pores present in both phases has been also considered, as it may provide important indications on the actual formation mechanism of hematite.

Keywords Iron oxide · Phase transformation · Thermogravimetry · X-ray diffraction · Raman spectroscopy · Transmission electron microscopy

Introduction

Hematite and other transition metal oxides display features and properties that make them attractive in many respects, related to fundamental science and technological applications [1, 2]. The search for novel and efficient processing routes has stimulated research efforts for understanding the mechanisms of the transformations that, starting from precursor systems based on hydroxides, would lead, through suitable thermal treatments, to more stable oxides, carbonates, and other similar phases [3]. As to hematite, a further point of interest is related to its use as a red pigment since prehistoric ages, in primitive cave paintings [4], through more recent periods [5], until present. The widespread diffusion of these red color materials can be ascribed to the ubiquitous presence of iron oxides, which mostly derive from the aerobic weathering of surface layers of magmatic rocks.

In this study, a multianalytical experimental approach is used for the characterization of the changes, as concerns crystalline structure and microstructure, observed during the thermally induced transformation of goethite ($\alpha\text{-FeOOH}$) into hematite ($\alpha\text{-Fe}_2\text{O}_3$). A general interest in this transformation is related to the use of natural raw materials for industrial processes and technological purposes. This concerns not only hematite in itself but also those minerals, such as, for instance, bauxite, containing hematite as a second phase, that can be thus profitably used to characterize the thermally activated state of the hosting mineral [6]. Moreover, the findings of the present study are discussed in

S. Gialanella (✉) · F. Girardi · G. Ischia · I. Lonardelli
Dipartimento di Ingegneria dei Materiali e Tecnologie
Industriali, Università degli Studi di Trento, Mesiano,
Trento 38050, Italy
e-mail: stefano.gialanella@ing.unitn.it

M. Mattarelli · M. Montagna
Dipartimento di Fisica, Università degli Studi di Trento,
Povo, Trento 38050, Italy

connection to their archaeological implications, which will be fully developed in a future study.

Experimental

Natural hematite or goethite samples are always found with significant concentration of impurities, present as trace or minority chemical elements (aluminum and titanium ions are frequently found in the place of iron ions) and secondary phases. Of course, these impurities have effect on the phase transition occurring upon heating goethite samples, as shown by several studies [3, 7]. The impurity issue is particularly important when dealing with natural raw materials, like those that can be found in archaeological sites. Therefore, it was decided to conduct the experimental tests discussed herewith on two goethite samples of different grades. A commercial goethite powder, codenamed “SA” (Sigma-Aldrich, Goethite—CAS No. 20344-49-4; ca. 35% wt Fe; note that for pure goethite, Fe concentration would be 63% wt), containing a significant fraction of impurities, mainly in the form of magnesium, silicon, calcium, and aluminum oxides, as specified in the technical data sheet of the product. The other investigated material was a natural goethite (codenamed “GS”), in which, XRD analysis, not reported herewith, revealed that a concentration of about 10 wt% silicon oxide (quartz), a phase that is commonly found in natural goethite. A commercial hematite (BDH Chemicals) with 95% purity was also considered as a reference sample.

Differential thermal analysis (DTA) and thermogravimetry (TG) tests were conducted on the goethite samples, to evaluate the relevant transition temperatures and transformation mechanisms. Continuous heating and cooling scans were performed on goethite powder samples, under a flux of dry air, from 20 °C up to 1,000 °C with a heating and cooling rate of 10 °C/min.

Structural evolution and phase transformation of goethite and hematite were monitored by synchrotron powder diffraction at the high resolution ID31 beam-line of the European Synchrotron Radiation Facility in Grenoble, France. Capillary spinning on the axis of diffractometer was used to minimize preferred orientation due to the alignment of the sample along capillary axis and also to improve statistics. Samples were heated using a hot air blower, which allows reaching 1,000 °C. Analyses were carried at room temperature and, starting from 150 °C, every 25 °C up to 975 °C for the SA material (Sigma-Aldrich) and starting from 175 °C every 15 °C up to 985 °C for GS goethite. A heating rate of 10 °C/min was used. Moreover, an isothermal stay at the set temperature of 2 min was performed before starting each measurement for a better thermal stabilization. Experiments were carried out using a fixed X-ray wavelength

$\lambda = 0.7999 \text{ \AA}$. In order to evaluate the instrumental contribution to diffraction peak shape, a silicon standard NIST 640c was used. All experimental data were analyzed using the Material Analysis Using Diffraction (MAUD) software package [8], an original software used to work out quantitative crystallographic and microstructural information using a Rietveld code, exploiting the entire diffraction pattern for quantitative phase analysis (QPA) and line profile analysis (LPA) [9].

The indications provided by the thermoanalytical tests were used to select the temperatures for treating a set of goethite samples, taken from the SA and GS lots. Thermal treatments were conducted in air, at the following temperatures: 200, 300, 400, 600, 800, and 1,000 °C. Each sample was kept at the set temperature for 1 h and then air-cooled down to room temperature.

Powder samples in the initial condition and after annealing treatments were prepared for transmission electron microscopy (TEM) observations. A little amount of each sample was suspended in ethanol using an ultrasonic bath to get rid of agglomeration. A drop of this suspension was deposited onto a carbon coated copper grid. Images of the microstructure and the relevant selected area electron diffraction (SAED) patterns were acquired using an analytical electron microscope, operated at 120 keV. SAED patterns were indexed with the software package described in [10].

Raman spectroscopy (RMS) measures upon 632.8 nm excitation were collected by means of a microRaman single grating spectrometer. The polarization of the collected spectra was not defined. The measurements were performed with low power of excitation (about 0.02 mW, on a $5 \mu\text{m}^2$ region) to avoid a significant laser heating of the samples. The resolution, as obtained from the measure of Rayleigh line, was 2 cm^{-1} . The parameters of the spectra were extracted by fitting the Raman peaks to Lorentzian curves, after subtracting the background contribution due to luminescence.

Results and discussion

From goethite to hematite: thermoanalytical aspects

The DTA curves in Fig. 1 display, as more intense endothermic peaks, those pertaining to the phase transition from goethite to hematite, occurring during the first heating run of the two goethite materials (SA and GS). This irreversible transformation occurs, as expected [3, 6, 7, 11–14], over a temperature range centered around 300 °C. The features of the relevant thermoanalytical signals were influenced by microstructural and compositional factors. In particular, the GS material displays a single endothermic peak, comparatively sharp and with a peak temperature of 344 °C. This temperature is definitely higher than the peak temperature

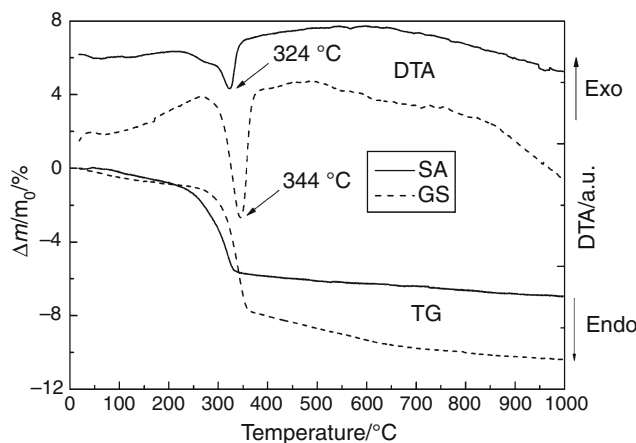


Fig. 1 DTA and TG curves for the two goethite materials (SA and GS) considered in the present investigation

for the SA material, equal to 324 °C. Moreover, the transformation signal in the SA material is clearly split into two contributions, at least: a lower temperature peak appears as a shoulder of the more intense one. This two-step transformation of goethite has been reported in other investigations and can be due to the actual chemical composition and microstructure of the analyzed goethite [3, 14]. A small-sized goethite, with a high specific surface area, would generally feature a single peak transition, occurring at lower temperatures [14]. Two DTA peaks would appear instead of larger grain size, in which case, the water escaping from the goethite lattice, as a consequence of the thermal treatments, may follow different paths and, thereby, the process may have different activation energies. A double peak in the DTA curves may even be determined by the presence of substitutional, such as Al atoms and other contaminants, in the goethite lattice [3].

Composition and microstructure will influence the kinetics of the de-hydration of goethite, i.e., in fact, the transformation recorded by the DTA curves and described by the following reaction:



with a water release equal to 10.1 wt%.

In both SA and GS materials, due to the presence of important fractions of secondary phases, lower mass losses have been obtained from the TG curves in Fig. 1. In particular, the SA material provides a total mass loss of 5.1%, a value that is slightly lower than what expected from the actual phase composition of this material, in which an initial concentration of goethite equal to 61 wt% is present (the rest 39% being a mixture of SiO₂, MgO, Al₂O₃, and other oxides). Thus, a complete dehydration would result in a mass loss equal to 6.0%.

The transformation kinetics of the GS sample displays a mass loss equal to 7.1% up to 350 °C approximately (Fig. 1).

The mass of the specimen continues to decrease further up to 730 °C, and the total amount of water that evolves from the transforming GS goethite would correspond to a 9.0% mass loss. This value is in excellent agreement with the phase composition of the GS material, in which an initial concentration of 90 wt% goethite has been estimated from the XRD data. If all of the starting goethite is transformed into hematite, the relevant mass change would exactly correspond to the recorded thermogravimetric datum.

From goethite to hematite: crystallographic and microstructural changes

Transformations occurring in the goethite powders when heated from room up to above the transition temperature have been characterized by in situ diffraction experiments. Some of the diffraction patterns obtained upon heating the GS sample are shown in Fig. 2. It can be seen how goethite reflections are progressively replaced by hematites. LPA has provided the relevant crystallite size and microstrain values, interesting to monitor the evolution of goethite first and, then, of hematite.

Coarsening of the coherently scattering domains occurs in an anisotropic way in goethite (Fig. 3). A monotonic trend along the [104] and [110] axes of hematite can be observed instead (Fig. 4a). It is worth noticing that, as soon as the fraction of hematite is such that its reflections are detectable, comparatively high microstrain values are measured. At 350 °C, microstrain falls down to a value that remains substantially the same up to 1,000 °C. This behavior is compatible with the release of the OH⁻ groups. The graph in Fig. 4b shows how the cell parameters of hematite change as a function of the annealing temperature. From a comparison with literature data for pure hematite

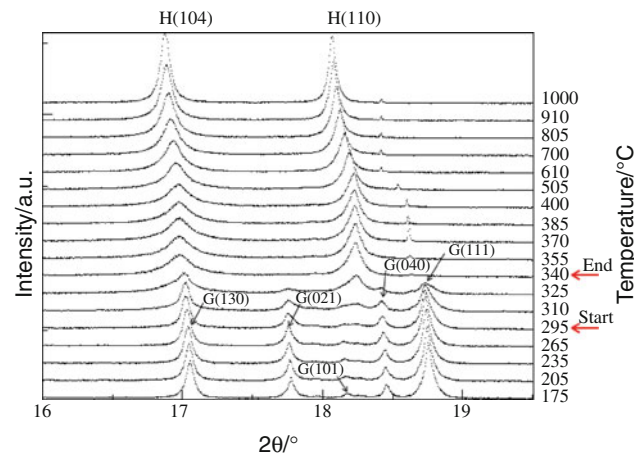


Fig. 2 Synchrotron radiation diffraction patterns displaying the evolution of the phase transformation of goethite (G-peaks) into hematite (H-peaks) as occurring during in situ heating experiments. GS material

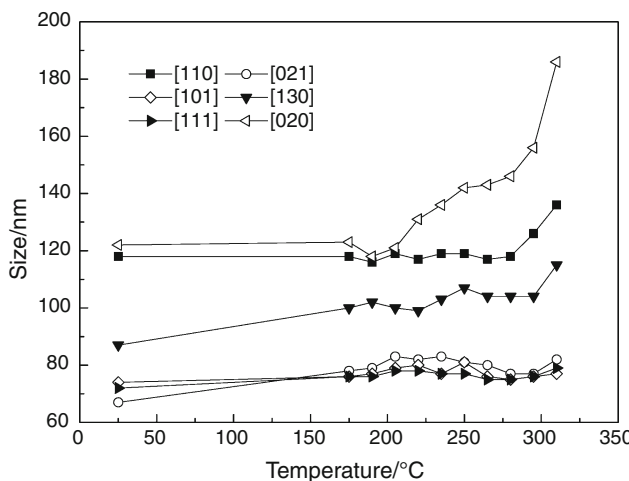


Fig. 3 Change of the average crystallite size along different directions in goethite, as a function of the annealing temperature, during in situ XRD measurements. GS material

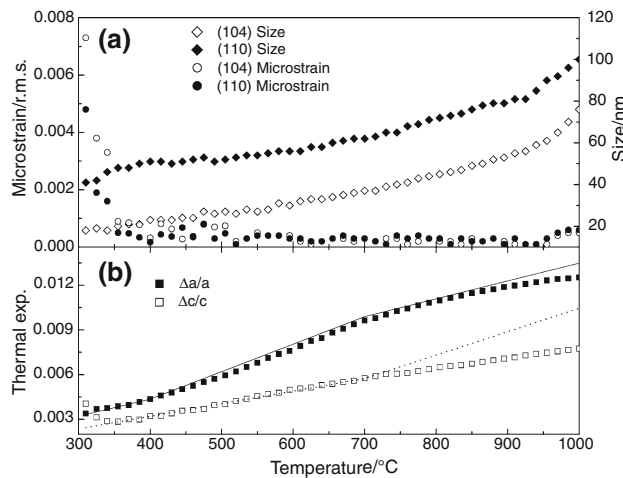


Fig. 4 **a** Changes of the average crystallite size and microstrain along [104] and [110] directions in hematite, as a function of the annealing temperature during in situ XRD experiments. Note the sharp decrease in microstrain just above the transition temperature (around 300 °C). **b** Thermal expansion of lattice parameters as a function of temperature during in situ annealing, compared with literature [15] data (solid and dotted lines) for pure hematite samples. GS material

[15], it turns out that the expansion of both parameters has substantially the same trend as the reference data, up to about 750 °C. At higher temperatures, the expansion of our defective sample (GS material) is smaller than that of the reference material. This indicates that the high temperature treatment produces an “anomalous” shrinkage of the cell parameters, a behavior that is determined by the phenomena going on at these temperatures, involving impurities and described in the following.

It should be noted that the α -FeOOH transforms into α -Fe₂O₃ with minor structural modifications, as expected for a topotactic transformation [16]. Therefore, α -hematite

will retain some microstructural and textural features of the parent phase (α -goethite). In particular, the hexagonally close-packed arrays of oxygen anions, which can be found in the parent goethite, are still there in the daughter hematite.

Another consequence of the particular character of the transition is the existence of specific crystallographic relationships involving axes and planes of the two phases. As concerns the crystallographic planes, the following relationship is valid: $\{130\}_G/\{140\}_H$ in agreement with the reported behavior of hydroxyl units during the transformation [11].

The anisotropic and intercalated microstructure of the transforming grains (see below) are such that any outward diffusion process is more or less favored according to the direction the mass transport takes within goethite grains. This aspect and the high concentration of microstructural defects, unavoidably present in the newly formed hematite, would agree with the proposed existence of an intermediate phase, proto-hematite, or hydro-hematite [7, 12, 14].

From goethite to hematite: ex situ approach

In order to characterize further the changes involved with the goethite to hematite phase transition, two sets of goethite samples, GS and SA, were thermally treated in a furnace and then analyzed with TEM and RMS. TEM data presented in this section refer to the GS samples only, as the SA material provided similar results. The starting goethite has the microstructure, as shown in Fig. 5, with elongated, prismatic grains, and a layered inner substructure. The thickness of each layer is 5 nm approx., and, as reported in [1], each pair of layers is joined by OH⁻ groups. In samples treated 1 h at 300 °C, grain shape and size of the newly formed hematite phase are still substantially the same as those of the original goethite, although the layered structure is better visible as a result of the

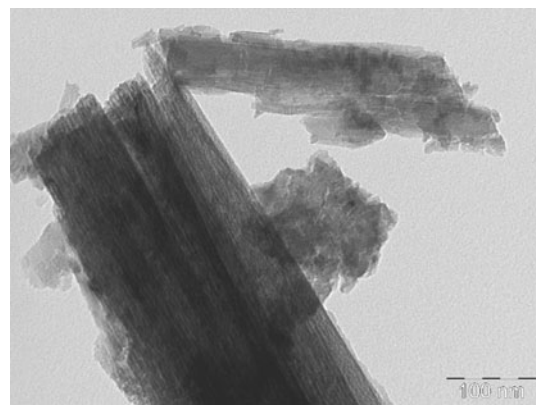


Fig. 5 TEM micrographs displaying the layered structure of goethite. GS material

release of the OH^- groups. Not even thermal treatments at 400 °C are significantly changing the situation. However, the structure of the hematite is locally loosing the initial regular pattern, as concerns the thickness and shape of intercalated layers. According to the TG data, at this temperature, most of the constitutional water molecules have been released. The outgoing flux of the OH^- groups and the contemporary diffusive rearrangement of the grain structure may determine local pile up of internal stresses, even capable to fracture the hematite grains.

In the specimens thermally treated at higher temperatures, the most evident changes produced by the diffusive phenomena concern the growth of increasingly spherical pores as shown in Fig. 6, referring to the sample treated at 800 °C. Driven by the tendency to reduce the surface energy contribution, closed spherical pores tend to replace the open intercalated structure, produced in the hematite grains by dehydration of goethite. The same driving force induces the smearing out of the initially sharp corners of the grains and their partial sintering, as shown by the TEM micrograph of the samples treated at 1,000 °C as shown in Fig. 7.

In Fig. 8, Raman spectra for the thermally treated GS samples are displayed. The spectrum of the 95% pure hematite powder (BDH sample) is also reported, for a comparison. The frequencies of the vibrational peaks of hematite (goethite) are indicated by vertical solid (dotted) lines. Goethite and hematite feature well distinguishable Raman spectra, so that the transition between the two phases can be easily followed. At 300 °C, the goethite spectrum is dominant, but a contribution from the hematite is already observable. The spectra of SA samples show a similar behavior, but, in agreement with the thermoanalytical data, the hematite contribution dominates the spectrum already in the 300 °C sample, with only minor goethite features still present.

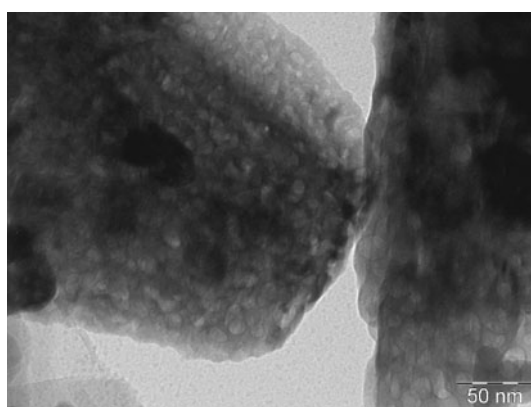


Fig. 6 TEM micrograph of hematite obtained from the thermal treatments of the GS goethite powder at 800 °C for 1 h. Changes in the shape and average size of the pores are visible

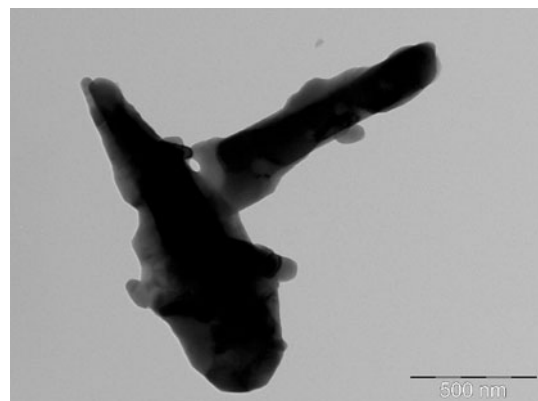


Fig. 7 TEM micrographs of the GS sample annealed for 1 h at 1,000 °C. General aspect of the hematite grains, displaying some degree of sintering

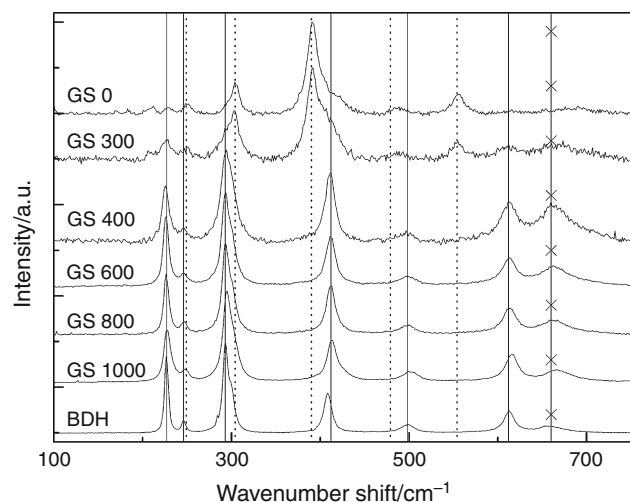


Fig. 8 Raman spectra upon 632.8 nm excitation of: GS goethite powders heat treated in air at temperatures ranging from 200 to 1,000 °C for 1 h. Vertical solid (dotted) lines indicate the positions of vibrational peaks of hematite (goethite). The 660 cm^{-1} peak, evidenced by crosses, would be absent in a pure hematite single crystal sample (see text). BDH spectrum refers to the hematite standard

The 660 cm^{-1} peak in the Raman hematite spectrum is not Raman active in a pure infinite crystalline domain, as its presence is rather due to the contribution of the chemical impurities and of the surface, where the cell symmetry breaks down [17]. All peaks are much broader than those of the reference sample (BDH) and in this case, the 660 cm^{-1} peak is relatively weak, indicating less defective crystallites. Moreover, the Raman peaks present some shift, which is strictly related to their broadening, in the sense that both shift and line-width tend to decrease as the annealing temperature increases.

The broadening of the Raman peaks can be mainly related to the presence of chemical impurities and

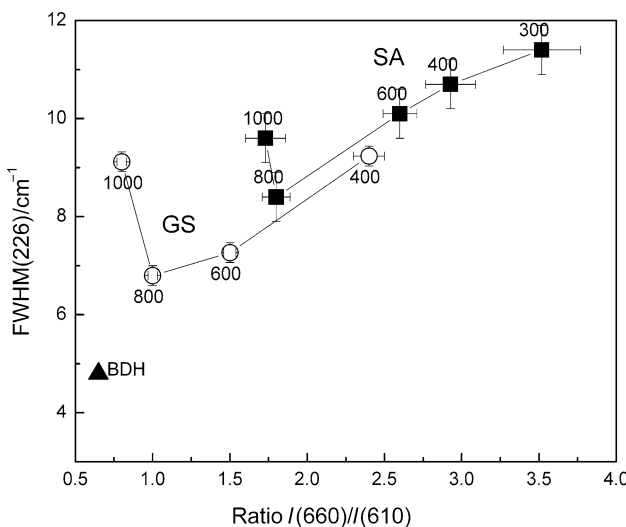


Fig. 9 FWHM of the 226 cm^{-1} peak as a function of the intensity ratio of the 660 cm^{-1} and 610 cm^{-1} peaks of the commercial (SA) and natural (GS) hematite samples

microstructural defects [18]. In Fig. 9 the full-width at half maximum (FWHM) of the peak at 226 cm^{-1} is displayed as a function of the intensity ratio $I(660)/I(610)$ ratio for the SA and GS samples in the initial and thermally treated conditions. The decreasing trend of the line-width, with increasing treatment temperature, up to $800\text{ }^{\circ}\text{C}$, is induced by the loss of OH^- groups, which, on abandoning the material, have the same effect as the reduction of the actual number of impurities. On the other hand, at $1,000\text{ }^{\circ}\text{C}$, we have a sudden increase of the line-width, and a shift to higher wavenumbers, while the intensity of the defect peak (660 cm^{-1}) decreases slightly. This would indicate that at least two different kinds of defects are present. As observed in TEM images, at $1,000\text{ }^{\circ}\text{C}$, hematite grains are fully recrystallized and partially sintered (Fig. 7). The intensity of the 660 cm^{-1} peak is influenced by surface contribution, that is progressively reduced for annealing temperatures as high as $800\text{ }^{\circ}\text{C}$.

The increase of the Raman line-widths after the heat treatment at $1,000\text{ }^{\circ}\text{C}$ indicates the presence of another active physical mechanism that can be interpreted as strains within the hematite grains associated with chemical impurities diffusing inside the recrystallizing grains. The substitution of iron ions with iso-electronic cations, such as Al^{3+} or Cr^{3+} , having smaller ionic radii ($\text{Fe}^{3+} = 65\text{ pm}$, $\text{Cr}^{3+} = 62\text{ pm}$, and $\text{Al}^{3+} = 54\text{ pm}$), is a reasonable explanation for this effect [19]. This would be in agreement with the increase of the frequency observed upon raising the annealing temperature from 800 to $1,000\text{ }^{\circ}\text{C}$ [20], which can be explained by an increase of impurities, with an estimated concentration in the 1–5%, depending on the actual atomic species. In this case, aluminum ions are the most effective, as they result in the higher hematite lattice contraction. Accordingly, as shown by Fig. 4b, although

the thermal expansion curves of our low purity samples are increasing to the same extent as those of a standard high purity hematite [15], they remain below this reference sample above $750\text{ }^{\circ}\text{C}$. The lower recorded expansion is determined by the contraction of crystal lattice induced by the inward diffusion of substitutional impurities that partially counterbalances the thermal effect.

Conclusions and further developments

This study has investigated the crystallographic and microstructural changes that occur and promote the thermally induced transformation of goethite into hematite. The multianalytical approach, that has been adopted, has afforded indications about these changes and the mutual influence they have on the resulting kinetics of the phase transition.

The first step of the transformation is the release of the OH^- groups that induces a progressive change of the crystalline structure. The newly formed hematite lattice is inherently quite defective. A further contribution, that renders hematite obtained from goethite defective, is the strain effects induced by the microstructural constraints. In fact, hematite (daughter phase) retains specific crystallographic relationships with goethite (parent phase), with a substantial lack of recrystallization of the original goethite grains, whose shape remains substantially unchanged in hematite, unless annealing temperatures in excess of $600\text{ }^{\circ}\text{C}$ are used. The good correlation between XRD and TEM data with the RMS results confirms that the size–shape effect of the crystalline grains plays an important role in this phase transition.

At temperatures above $800\text{ }^{\circ}\text{C}$, recrystallization and grain coarsening occurs. However, the relevant decrease of the size effect, due to the presence of high concentrations of impurities, is partially counterbalanced by the diffusion of substitutional atoms into the hematite lattice, thus producing a further increase of the structural disorder, clearly evidenced by the trend of the intensity ratios of RMS lines.

The evolution of the size and shape of pores is another parameter involved with the transformation and it seems to be suitable to investigate thermally induced changes. This aspect, that seems to be particularly sensitive to the transformation conditions [21, 22], would provide an interesting and effective approach to tackle the issue, mentioned in the “Introduction” section and often faced in archaeological investigations, of assigning an actual origin to hematite found in artifacts, such as cave and wall paintings, decorations, etc. [23, 24]. In fact, the comparatively low transition temperatures, that can be easily achieved even with the heat of camp fires and of other similar, not particularly complex, pyrotechnological processes, might leave some

degree of uncertainty about the original color of an artifact, the natural or artificial origin of hematite and similar issues. According to the results presented herewith, some of these questions might be clarified looking at the microstructure of the involved hematite, particularly its grain shape and the geometry of the pores.

Acknowledgements We thank the Provincia Autonoma di Trento for financial support through the Projects: PAT-CRS2006 (DIGITEM); MATIS; PAT-CRS2008 (Analisi micro-Raman di materiali).

References

- Trassati S. Transition metal oxides: versatile materials for electrocatalysis. In: Lipkowski J, Ross P, editors. *Electrochemistry of novel materials*, vol. III. Weinheim, Germany: VCH Verlagsgesellschaft; 1994. p. 207.
- Busca G, Daturi M, Finocchio E, Lorenzelli V, Ramis G, Willey RJ. Transition metal mixed oxides as combustion catalysts: preparation, characterization and activity mechanisms. *Catal Today*. 1997;33:239–49.
- Cornell RM, Schwertmann U. The iron oxides. Weinheim, Germany: VCH Verlagsgesellschaft; 1996.
- Marean CW, Bar-Matthews M, Bernatchez J, Fisher E, Goldberg P, Herries AIR, et al. Early human use of marine resources and pigment in South Africa during the Middle Pleistocene. *Nature*. 2008;449:905–8.
- Colombo L. Il colore degli antichi. 2nd ed. Florence: Nardini; 2003.
- Ruan HD, Frost RL, Kloprogge JT, Duong L. Infrared spectroscopy of goethite dehydroxylation: III. FT-IR microscopy of in situ study of the thermal transformation of goethite to hematite. *Spectrochim Acta A*. 2002;58:967–81.
- Ruan HD, Frost RL, Kloprogge JT, Duong L. Infrared spectroscopy of goethite dehydroxylation. II. Effect of aluminium substitution on the behaviour of hydroxyl units. *Spectrochim Acta A*. 2002;58:479–91.
- Lutterotti L, Matthies S, Wenk HR, Goodwin M. Combined texture and structure analysis of deformed limestone from time-of-flight neutron diffraction spectra. *J Appl Phys*. 1997;81:594–600.
- Lonardelli I, Wenk HR, Lutterotti L, Goodwin M. Texture analysis from synchrotron diffraction images with the Rietveld method: dinosaur tendon and salmon scale. *J Synchrotron Radiat*. 2005;12:354–60.
- Labar JL. Consistent indexing of a (set of) single crystal SAED pattern(s) with the process diffraction program. *Ultramicroscopy*. 2005;103:237–49.
- Ruan HD, Frost RL, Kloprogge JT. The behavior of hydroxyl units of synthetic goethite and its dehydroxylated product hematite. *Spectrochim Acta A*. 2001;57:2575–86.
- Gualtieri AF, Venturelli P. In situ study of the goethite-hematite phase transformation by real time synchrotron powder diffraction. *Am Mineral*. 1999;84:895–904.
- Hongley F, Song B, Li Q. Thermal behavior of goethite during transformation to hematite. *Mater Chem Phys*. 2006;98:148–53.
- Walter D, Buxbaum D, Laqua W. The mechanism of the thermal transformation from goethite to hematite. *J Therm Anal Calorim*. 2001;63:733–48.
- Saito T. The anomalous thermal expansion of hematite at a high temperature. *Bull Chem Soc Jpn*. 1965;38:2008–9.
- Ocaña M, Morales MP, Serna CJ. The growth mechanism of α -Fe₂O₃ ellipsoidal particles in solution. *J Colloid Interface Sci*. 1995;171:85–91.
- Bersani D, Lottici P, Montenero A. Micro-Raman investigation of iron oxide films and powders produced by sol-gel syntheses. *J Raman Spectrosc*. 1999;30:355–60.
- Gouadec G, Colomban P. Raman spectroscopy of nanomaterials: how spectra relate to disorder, particle size and mechanical properties. *Prog Cryst Growth Charact Mater*. 2007;53:1–56.
- Housecroft C, Sharpe AG. *Inorganic chemistry*. Harlow: Prentice Hall; 2007.
- Massey MJ, Baier U, Merlin R, Weber WH. Effects of pressure and isotopic-substitution on the Raman-spectrum of alpha-Fe₂O₃—identification of 2-magnon scattering. *Phys Rev B*. 1990;41:7822–7.
- Pelino M, Toro L, Petroni M, Florindi A, Cantalini C. Study of the kinetics of decomposition of goethite *in vacuo* and pore structure of product particles. *J Mater Sci*. 1989;24:409–12.
- Rendon JL, Cornejo J, De Aramburu P, Serna J. Grinding-induced effects on goethite (α -FeOOH). *J Colloid Interface Sci*. 1983;92:508–16.
- de Faria DLA, Lopes FN. Heated goethite and natural hematite: can Raman spectroscopy be used to differentiate them? *Vib Spectrosc*. 2007;45:117–21.
- Frost RL, Ding Z, Ruan HD. Thermal analysis of goethite. Relevance to Australian indigenous art. *J Therm Anal Calorim*. 2003;71:783–97.